MECH. RES. COMM. Vol.1, 225-231, 1974. Pergamon Press. Printed in USA.

FRACTURE INITIATION AND PROPAGATION IN ELASTIC BRITTLE MATERIALS SUBJECTED TO COMPRESSIVE STRESS FIELDS - AN EXPERIMENTAL STUDY

N.J. Altiero and D.L. Sikarskie
Department of Aerospace Engineering, The University of Michigan
Ann Arbor, Michigan, U.S.A.

(Received 2 July 1974; accepted as ready for print 10 July 1974)

Introduction

In a series of previous papers [1, 2, 3] a theory has been outlined for the initiation and propagation of macrofracture in elastic brittle materials subjected to nonhomogeneous compressive stress fields. In the present paper this theory is examined experimentally. Results show excellent agreement with the predicted fracture initiation location and force levels and reasonable agreement with the predicted fracture propagation.

The linear theory, as developed in [1, 3], defines a fracture function:

$$F(\sigma_1, \sigma_2; \mu) = \frac{\mu}{2}(\sigma_1 + \sigma_2) + \frac{\sqrt{1+\mu^2}}{2}(\sigma_1 - \sigma_2) \tag{1}$$

$$\sigma_1 = \bar{\sigma}_1 L/P \qquad\qquad \sigma_2 = \bar{\sigma}_2 L/P$$

where $\bar{\sigma}_1$, $\bar{\sigma}_2$ are dimensional principal stresses with $\bar{\sigma}_1 > \bar{\sigma}_2$ and μ is the slope of the envelope of a set of Mohr circles defining strength failure of the material [4]. Stresses are nondimensionalized with respect to P, L where P represents the total force and L the characteristic length shown in Figure (1). Fracture initiates in the field where $F(\sigma_1, \sigma_2; \mu)$ is maximized and when the stresses are such that

$$F(\sigma_1, \sigma_2; \mu) = \boldsymbol{\beta} = CL/P_I \tag{2}$$

where C is the $\bar{\tau}$ (shear stress) intercept of the strength failure envelope (cohesion) and P_I is the fracture initiation load. Fracture propagation is considered to be a succession of fracture initiations [1, 3], i.e., the microfractures emanating from critically oriented Griffith flaws coallesce to form the final fracture path; the macrofracture.

Scientific Communication

Analysis

The boundary value problem to be analyzed (and subsequently studied experimentally) is that shown in Figure (1).

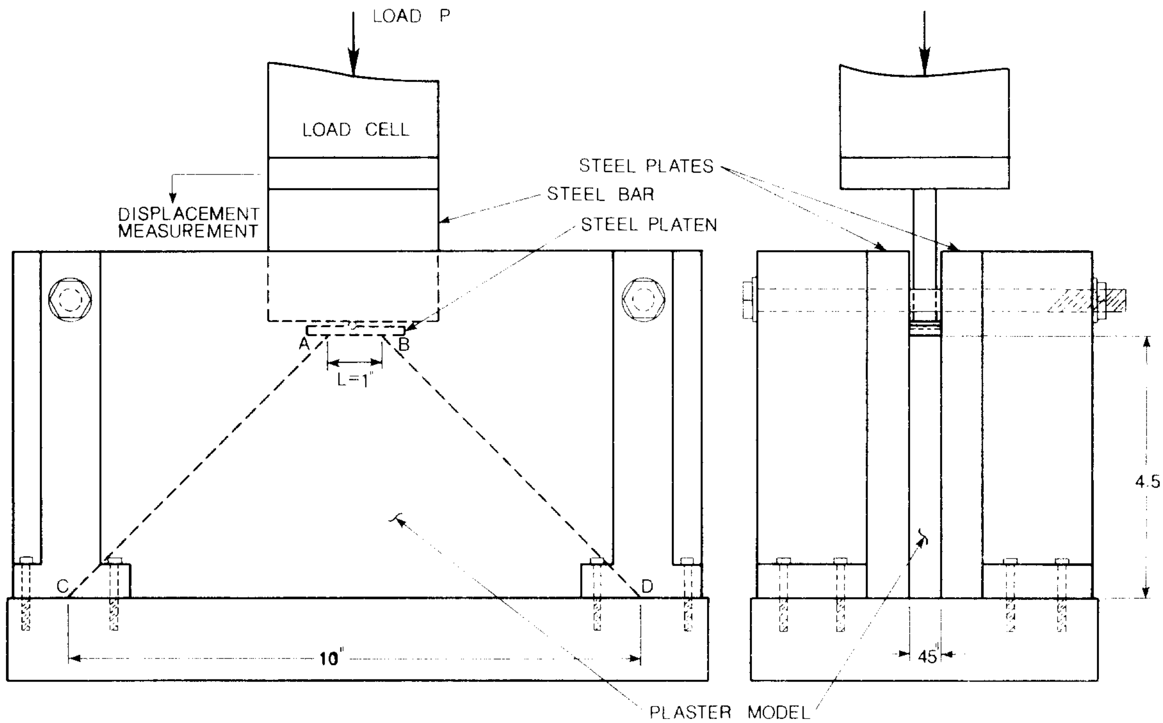

FIG. 1
Plaster Model in Loading Fixture

This is a mixed problem; i.e., zero traction on DB and AC, specified vertical displacement and zero shear stress on BA and CD. An integral equation procedure particularly convenient for fracture analysis and described in detail in [3, 5, 6] is used to obtain the stress field σ_1, σ_2. The material studied experimentally was a modeling plaster having the following material constants:[1]

$$E = 4.2 \times 10^5 \text{ psi}$$
$$\nu = .24$$
$$C = 590 \text{ psi}$$
$$\mu = .93$$

[1] These constants were determined using standard tests and test specimens made and cured under the same conditions as the model specimens.

Results of the analysis are shown in Figure (2). Fracture here initiates in the corners A, B of the specimen. This is due to the large normal traction components at the corners caused by the uniform displacement of the surface BA. For P increasing and greater than P_I, $F(\sigma_1, \sigma_2; \mu) = \beta$ represents a growing contour within which microcracking (damage) is occurring. It is postulated that the direction of macrofracture growth is coincident with the maximum

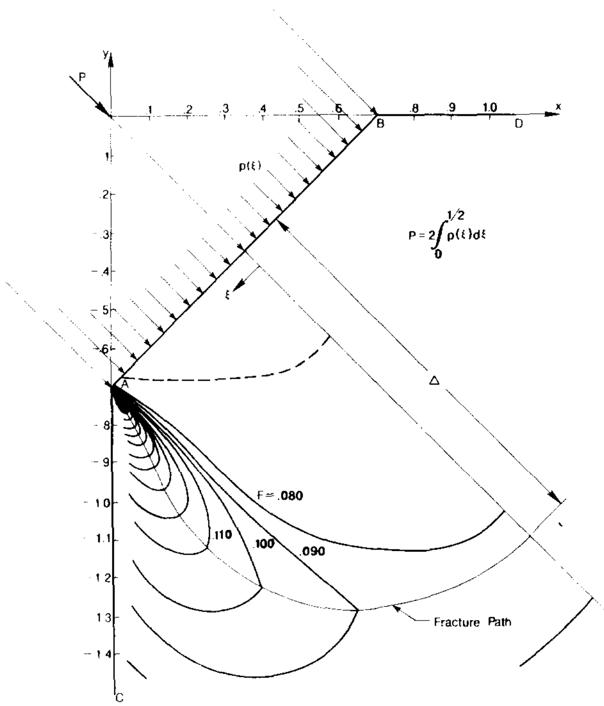

FIG. 2
Contour Map for Plaster;
Uniform Displacement of BA

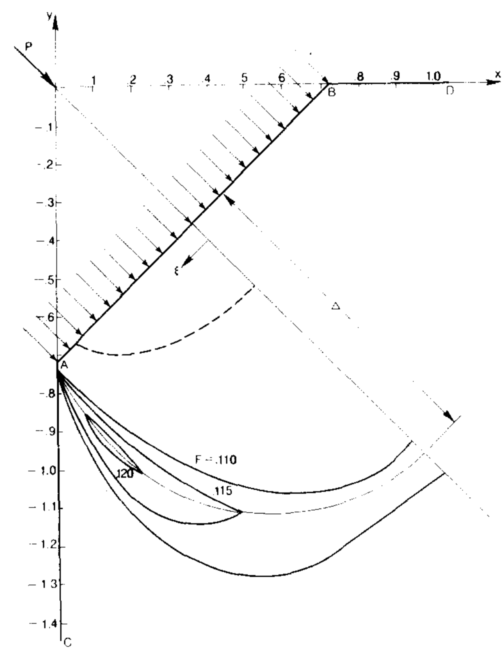

FIG. 3
Contour Map for Plaster;
Uniform Traction Along BA

growth direction of this contour. The contour map shown in Figure (2) represents a discretized approximation of this contour growth with a predicted macrofracture path as shown. It is approximate because it is based on the stress state in the undamaged material. Note that there is no approximation for fracture initiation load, location and initial direction. As macrofracture progresses beyond the initiation point, the stress field (and surface traction distribution) changes and the approximation becomes poorer.[2] A second

[2] The microfracturing occurring within the initiation contour $F(\sigma_1, \sigma_2; \mu) = \beta$ introduces dilatancy which has a marked effect on the surrounding stress field. Work is in progress on determining the stress field in the presence of such damage. When complete, no stress field approximation will be necessary.

boundary value problem, i.e., uniform normal surface traction, is also considered and the results are presented in Figure (3). Due to the initial direction of macrofracture propagation, normal to the loaded surface, it is felt that this represents a better approximation to final chip depth and formation load. Numerical results for both the uniform displacement and uniform traction cases are given in Table I.

Experimental Results

The experimental apparatus is shown in Figure (1). The models were confined between two steel plates to insure plane strain conditions. Double layers of .005" thick Teflon sheets were placed between the steel plates and the model faces and between the steel platen and loaded surface BA to eliminate shear forces due to friction. The boundary conditions on face BA, therefore, consisted of a uniform vertical displacement and zero shear traction. The load was applied quasi-statically (50 pounds per second). Total load on the surface BA was measured with a B. L. H. model U3G1 load cell while the vertical displacement was measured with a Shaevitz model 500 HR L.V.D.T. Load displacement plots were recorded on a Hewlett-Packard X-Y plotter; see, for example, Figure (4).

Test specimens were made of a medium set modeling plaster, an elastic brittle material which is often used to simulate rock [7,8]. To insure brittle behavior, the plaster-water ratio chosen was low (70 parts by weight of plaster to 100 parts by weight of water). Tap water at a temperature of 60°F was used. The plaster-water mixture was stirred until all air bubbles were removed and the mixture had begun to thicken (10 minutes). The models were cast in aluminum molds which had been greased to facilitate removal. The mixture hardened in 15-20 minutes and was then removed from the mold. The models were cured at room temperature (70°F) for six months. They were stored in an upright position during this time. Prior to testing, the models were carefully machined to insure flat, smooth faces and a uniform thickness (.450").

Experimental results are presented in Table I and Figures (4,5). Fracture

TABLE I
Results

	Test No.	Fracture Initiation Load P_i (pounds)	Chip Formation Load P_f (pounds)	Depth Δ (inches)
Experimental Results	1	1030	1400	.65
	2	1125	1500	.65
	3	1250	1525	.65
	4	1050	1400	.60
	5	1160	1575	.60
	6	1050	1600	.60
	7	1200	--	--
	8	1180	1500	.55
	Average	1130	1500	.61
Theory	Uniform displ.	1070	3200	1.00
	Uniform traction	--	2400	.80

initiation and growth of the damage region (to form the final macrofracture) are evidenced in Figure (4). For increasing load the specimen behaves in a linear elastic manner up to point I. At point I fracture initiates at the corners A, B in Figure (2). The location and direction of initiation were determined experimentally by stopping the test just beyond point I and observing the fracture. Results are in agreement with the theoretical predictions, i.e., Figure (2). From point I to II microdamage occurs in two separate regions emanating from points A, B on Figure (2). At point II these regions meet. This was determined by stopping the test at this point and carefully removing the completed chip, see Figure (5). The portion of the curve from points II to III represents the action of forcing the completed chip into the cavity. Tensile stresses are introduced

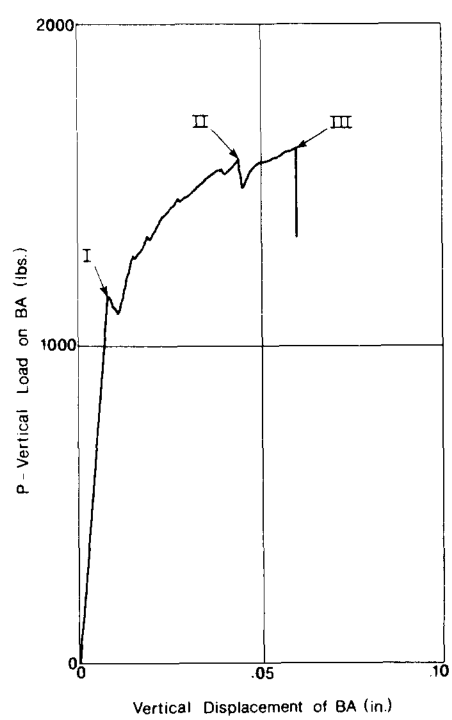

FIG. 4
Typical Force-Displacement Plot of Uniform Displacement Test on Plaster Model (Test No. 5)

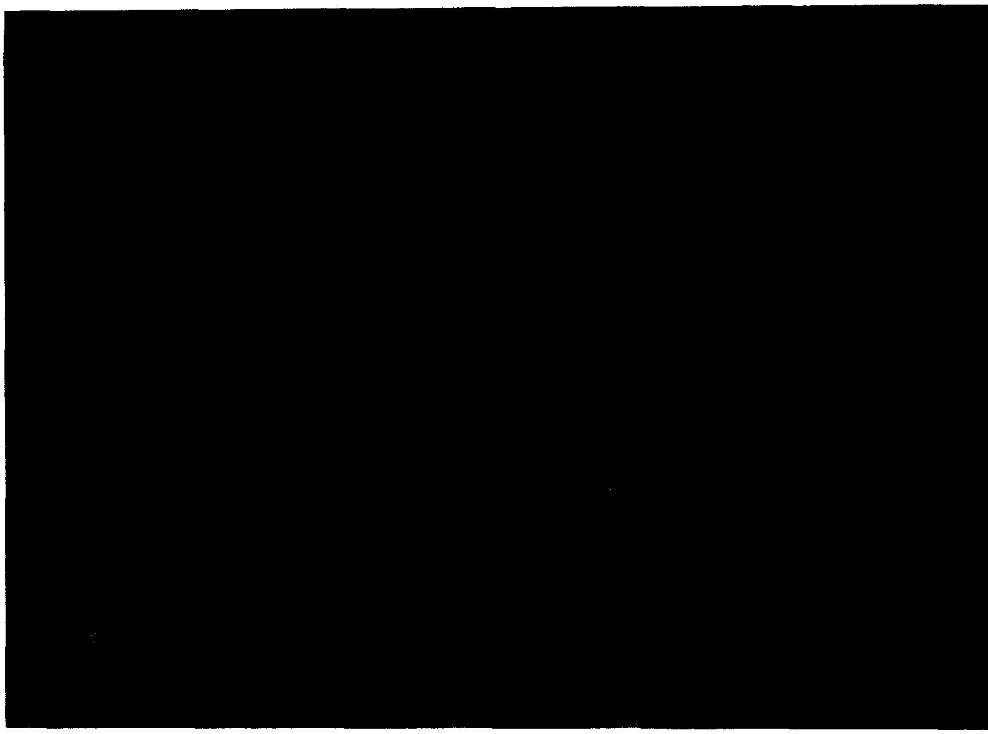

FIG. 5
Photograph of Complete Chip

at the base of the cavity and, at III, a mode I (tensile) fracture emanates from this point, splitting the model. Numerical results are presented in Table I. The average of the initiation loads is within 7% of the predicted value. The chip formation load and chip depth are in poorer agreement as expected due to the use of the prefracture stress field. As discussed previously, it is felt that the uniform traction case provides a better approximation for the ultimate chip characteristics. This is evident in Table I.

Dotted lines are shown on Figures (2,3) near the surface BA. These lines represent regions in which the intermediate principal stress is not normal to the specimen plane (under plane strain conditions and for $\nu = .24$, see [3]). This introduces the possibility of oblique fracture in this region. Such fractures were observed experimentally.

While much additional work is yet to be done in refining both the theoretical predictions and the experimental observation of fracture growth (both micro and macro), the results presented show significant promise.

References

1. D.L Sikarskie and N.J. Altiero, "The Formation of Chips in the Penetration of Elastic-Brittle Materials (Rock)," J. Applied Mechanics 40, 3, Trans. ASME 95, p. 791 (1973).

2. N.J. Altiero and D.L. Sikarskie, "Fracture Initiation in Elastic-Brittle Materials Having Nonlinear Fracture Envelopes," to appear in Intl. J. Fracture (1974).

3. N.J. Altiero, Fracture Initiation and Propagation in Nonuniform Compressive Stress Fields, doctoral dissertation, Univ. of Michigan (1974).

4. W.F. Brace, "Brittle Fracture of Rocks," State of Stress in the Earth's Crust, ed. W. Judd, Elsevier, New York (1964).

5. C. Massonnet, "Numerical Use of Integral Procedures," Stress Analysis-Recent Developments in Numerical and Experimental Methods, ed. O.C. Zienkiewicz and G.S. Holister, J. Wiley, New York (1965).

6. R. Benjumea and D.L. Sikarskie, "On the Solution of Plane, Orthotropic Elasticity Problems by an Integral Method," Journal of Applied Mechanics 39, 3, Trans. ASME 94, p. 801 (1972)

7. B. Stimpson, "Modelling Materials for Engineering Rock Mechanics," Intl. J. Rock Mech. and Mining Sci. 7, p. 77 (1970).

8. K. Barron and G.E. Larocque, "Development of a Model for a Mine Structure," Proc. Rock Mech. Symp., McGill Univ., p. 145 (1962).